Hindawi
Journal of Chemistry
Volume 2019, Article ID 4121864, 15 pages
https://doi.org/10.1155/2019/4121864

Research Article

Removal Properties, Mechanisms, and Performance of Methyl Green from Aqueous Solution Using Raw and Purified Sejnane Clay Type

Yosra Satlaoui,[1,2] Mariem Trifi,[1,2] Dalila Fkih Romdhane,[2] Abdelkrim Charef,[2] and Rim Azouzi[2]

[1]*Department of Geology, Faculty of Sciences of Bizerte, 7021 Zarzouna-Bizerte, Tunisia*
[2]*Laboratory of Georesources, CERTE, Technopole Borj Cedria, 2073 Nabeul, Tunisia*

Correspondence should be addressed to Abdelkrim Charef; abdelkrim.charef@certe.rnrt.tn

Received 8 March 2019; Revised 21 June 2019; Accepted 25 June 2019; Published 21 August 2019

Academic Editor: Ana Moldes

Adsorption of cationic methyl green (MG) on nontreated (AB) and purified (AP) natural Sejnane clay type was studied in an equilibrium batch process. This work reported the application of kaolinite-rich heterogeneous clay for the removal of a cationic dye. Effects of contact time, initial dye concentration, mass adsorbent, pH, and temperature on the MG removal were checked. The adsorbent before and after adsorption processes was characterized by X-ray diffraction (XRD), scanning electron microscopy (SEM), Fourier transform infrared (FTIR), and atomic adsorption spectrophotometer. Equilibrium data were mathematically modeled using the Freundlich, Langmuir, and intraparticle diffusion models. Kinetic of adsorption was determined by pseudo-first-order and pseudo-second-order models. The free energy (ΔG°), standard enthalpy (ΔH°), and standard entropy (ΔS°) were calculated. A fast increase in the equilibrium removal of the cationic dye was obtained at a pH ranging between 3 and 11 and moderate temperature. This rapid MG adsorption proved the efficiency of kaolinite clay in cationic dye removal. Decolorizing yields were 73.3% for AB and 99.8% for AP. Thus, the adsorption capacity of purified clay was clearly higher than of H_2SO_4 and thermic activated clays. The data more closely resembled a pseudo-second-order model process, and the clay had reasonable Freundlich adsorption capacity. Adsorption process was endothermic and spontaneous chemisorption. SEM analysis showed that the adsorbed MG had remarkably changed the morphology of raw and purified clay surface. The low desorption rates confirmed effectiveness of this type of material for the retention of methyl green molecules. Thus, tested clays have no environmental impact.

1. Introduction

The use of dyes in various fields, including textile industry, continues to increase. To ensure good quality and long product life, these industries use dyes that exhibit color stability and high resistance to abrasion, microbial degradation, and oxidation [1]. Their persistent characteristics and the complexity of their molecules mean they are classed as major pollutants [2]. Thus, discharges of colored effluents released into the wild pose a dramatic threat that leads to the deterioration of ecosystems by generation of eutrophication and may even threaten aquatic and human life by bioaccumulation. In order to deal with this problem, their treatment is essential.

Triphenylmethane dyes are consumed extensively in various industries to color textile, cosmetic, and plastic products. They are also used in leather and food industries [3]. Methyl green (MG) is a cationic triphenylmethane used in medicine [4] and for sensitization of gelatinous films [5].

MG elimination has been object of multiple studies, such as MG elimination by photodecolorization [6, 7], UV photolysis [8], biodegradation [9], and adsorption on activated carbon [10], graphene sheet [11], and activated bentonite [12].

Clays presented a laminated structure, fine particle size, large surface area, and high cation-exchange capacity. These characteristics allow them to be considered as good pollutant adsorbents [13]. These materials that are available, nontoxic, and not expensive are increasingly used in dyes removal from wastewater.

Due to their properties cited above, several clays with different mineralogies have been tested for removal by adsorption of multiple dyes. Untreated or modified clays were tested for the removal of cationic [12, 14–16] and anionic dyes [14, 17–19]. Clay dominated or containing smectite has shown a high efficiency in the retention of dyes [17, 20]. Recent studies have highlighted the bleaching power of kaolinite clay [14, 20].

Pure clays are more expensive and increasingly rare. Thus, industrials have resorted to the heterogeneous clay compositions. These deposits have very variable mineralogical and geochemical compositions as well in a same field and in two deposits that have comparable geological contexts. Thus, whatever the deposit, a detailed study should be made initially on the one hand to characterize these materials and, on the other hand, to test the exact application of the selected deposit.

Tunisia has large quantities of clay materials and a well-known textile industry. The valorization of these resources for the discoloration of textile rejects has been subject of multiple studies. Tunisian clays, without treatment or modification, were tested for the removal of methyl blue [21], Reactive Red 120 [20, 22], and others (e.g., [23]). Investigation of the potential elimination of dyes with Tunisian clays was carried out with clays that have different mineralogical and chemical characteristics. Palygorskite-rich [23], smectite-illite-rich [24], kaolinite-illite-rich [20], and kaolinite-smectite-illite-rich [22, 25] clays and others were tested. These natural clays are clearly different by their clay proportions and their mineralogy and composition of the phyllosilicate and nonphyllosilicate fractions. Therefore, trying natural clays of Sejnane (northwestern Tunisia) that has different mineralogical and chemical compositions as an adsorbent support of MG aromatic dyes, which is excessively used in various industries [26], will provide accurate information on the ability and the efficiency of elimination of this dye by this type of clay.

Activated clays may better eliminate the textile dyes. Thus, comparison of adsorption capacity between, on the one hand, the raw and purified clays and activated clays with HCl, H_2SO_4, and temperature, on the other hand, is important. Also, it is interesting to compare the Sejnane clays' ability in MG elimination with some other materials and processes.

Therefore, our objective was the characterization of Sejnane clay before and after adsorption by XRD, FTIR, and SEM analyses, the identification of the MG removal capacity of these clay materials, and the optimization of the adsorption conditions. Adsorption of fairly high dye concentrations that exceeded 50 $mg \cdot g^{-1}$ on low clay mass was achieved in a batch system. Influence of initial dye concentration, adsorbent mass, pH, and temperature on the removal efficiency of this pollutant was determined. Thus, adsorption kinetics, isotherms, and thermodynamics of the process were presented. The experimental results obtained were compared with the results obtained for elimination tests of the same dye by activated Sejnane clay and other methods or using other adsorbents. Used clay contains a good fraction of carbonate and organic matter. To identify the role of these two fractions, adsorption capacity had been tested to judge whether it was desirable to purify clays prior to use. MG adsorption by clays helps clean the water. However, the saturated clays with MG could easily release their dyes. In this case, we just shifted the environmental problem. In order for this process to be effective, amounts of binding energy must be high to have a low desorption rate of MG. Therefore, desorption tests were carried out to evaluate the environmental risk of these loaded clays.

2. Materials and Methods

2.1. Sejnane Clay. Clay of the Sejnane region is an upper Oligocene autochthon series carried to the lower Serravallian series [27]. It is part of Jebel Louka, which is located in northern Tunisia. The UTM C coordinates of this site are E: 529590 and N: 4120268.

It is a layer of 270 m of clay that is a part of the Numidian Flysch. It is comparable to the basal turbiditic units of the Numidian described by Rouvier [27, 28]. It is bounded by a roof and a wall of quartz with some marl and marly limestone benches.

2.2. Sampling and Clay Characterization. Five (points) representative samples were taken from each plot (3×3 m). From each point, one volume of $10 \times 10 \times 20$ cm was taken. The five samples were homogenized, and an equivalent sample was passed through 2 mm stainless steel sieves. All samples were lyophilized and maintained at a temperature of about 4°C for the programmed analyses.

Grain size distribution (<63 μm) was assessed using wet sieving and the "Agregate Meter Laser" MAVERN X-ray grain size analyzer. Mineralogical composition of the total rock was identified by X-ray diffraction of a powder sample. For the preparation of pure clay fraction, the organic matter was removed with oxygenated water, and then, the carbonate fraction removal was obtained by an emersion of the sample in 0.1 N HCl. The operation was repeated several times until the total disappearance of effervescences. For the acid activation, samples were immersed in 0.5 to 4 N of boiling HCl or H_2SO_4 solutions, without stirring at 60°C for 3 h. All samples treated with HCl or H_2SO_4 solutions were subjected to a series of distilled water washings to remove the acid by centrifugation at a rate of 2500 rpm for 10 minutes and then dried at room temperature.

In order to study the effect of the thermal treatment of clay mineral on MG removal, the raw clays were heated in a furnace between 500°C and 1100°C for 2 h. The hot samples were cooled down to room temperature, dispersed in distilled water, and dried overnight at 50°C. The deflocculating of the suspension was done for the mineralogical analysis of clay fractions. Then, three oriented aggregate glass slides were prepared: (a) normal glass, (b) glass heated at 550°C for

2 h, and (c) glass treated with ethylene glycol. Mineralogy was identified with a SIEMENS D-5000 X-ray diffractometer with a scanning speed of 1°2θ min and Cu-Kα radiation (40 kV, 20 mA) [29, 30]. The semiquantitative estimation was based on the peaks' area and the chemical composition of the sample [31]. Chemical element concentrations were analyzed using an atomic adsorption spectrophotometer (AAS 200; PerkinElmer) with a graphite furnace and with inductively coupled plasma-mass spectroscopy (ICP-MS).

The appearance and morphology of material surface before and after adsorption was identified by scanning electron microscopy, and the EDX analysis was carried out with an SEM and its adjunct EDS analyzer (Thermoscientific Q250).

Specific surface area (SS) values were determined by the methylene blue spot method [32]. Cation-exchange capacity (CEC) was found using the Metson method (AFNOR, NF X 31-130). The Casagrande method [33–35] was selected for determining Atterberg limits of the clay. Experimental error was about ±3%.

AB and AP infrared spectra before and after adsorption were obtained by Fourier infrared spectroscopy [36, 37] using an FTIR spectrometer (Bruker FTIR-2000 spectrometer) with the reflection mode at a 4 cm^{-1} resolution in the 400–4000 cm^{-1} range.

2.3. Adsorbate and Adsorption Experiment. The tested adsorbate was methyl green which belongs to the large family of triphenylmethane dyes. It is a cationic and aromatic dye. The weight of its molecule is 458.47 g·mol^{-1}, and its empirical formula is $C_{26}H_{33}Cl_2N_3$ (Figure 1).

Adsorption experiments were carried out in batch system. A known dose of clay was introduced into 100 ml of colored water with given MG concentrations. The solution was stirred at a fixed speed of 450 rpm for 360 min. 5 ml of solution was collected at given time intervals. These samples were centrifuged at a speed of 3000 tr·min^{-1} for 20 min. To estimate the MG residual concentration, the supernatant was analyzed using a UV-Visible Perkin Elmer Lambda 25 spectrophotometer, at wavelengths between 200 and 800 nm. The remaining MG concentrations were measured using wavelength $\lambda = 632\,\mu$m.

The amount of the adsorbed dye was calculated by the following equation [37]:

$$\mathrm{Qt} = \left(C_0 - C_r\right) * \frac{v}{m}, \quad (1)$$

where Qt is the amount of dye per gram of the adsorbent (mg·g^{-1}); C_0 and C_r are, respectively, the concentrations of the initial and residual dye (mg·L^{-1}); v is the volume of the solution (L); and m is the mass of the used adsorbent (g).

In order to optimize the MG removal, effects of various factors were studied by varying one and fixing the others. Therefore, initial concentration (30 to 1000 mg·L^{-1}), contact time (0 to 360 min), clay mass (0.25 to 3 g), pH (3 to 11), and temperature (20, 30 and 40°C) were tested.

2.4. Modeling. Adsorption isotherms were used to determine the adsorption capacities of Sejnane clay and the type of adsorption (e.g., [38]). Langmuir and Freundlich adsorption models were used to identify the various adsorption systems. Isotherms were carried out for various dye concentrations. A fixed mass of clay (0.5 g) was contacted with different dye concentrations in 100 ml of solution. pH (5.2) and stirring solutions (6 hours) were fixed.

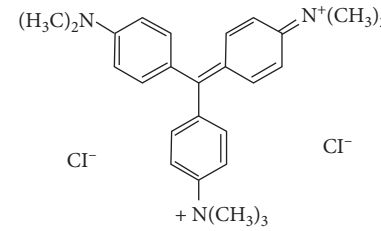

Figure 1: Structure of the molecule of methyl green.

For thermodynamic study, all parameters were fixed and just temperature was varied. Free energy (ΔG°), standard enthalpy (ΔH°), and standard entropy (ΔS°) were calculated. For the characterization of the adsorption phenomenon, modeling of adsorption kinetics was carried out by application of the pseudo-first-order and pseudo-second-order models.

To ensure accuracy and reproducibility of each obtained result, all sample analyses and batch equilibrium experiments were performed four times at least under identical conditions. The results were accepted only when the value stood below the detection limit or under 0.25% variation. Statistical analysis of the data was performed using STATISTICA version 6 software. Statistics-reported values were the arithmetic mean, maximum, minimum and standard deviation. To have simple representations, only mean values of batch experiments results were presented.

3. Results and Discussion

3.1. Clay Characterization

3.1.1. XRD and Chemical Analysis. Sejnane natural clay contained only 16.12% of clay (Table 1). Its chemical composition showed that this deposit was siliceous, aluminous, and rich in iron and characterized by a fine grain size (95% of the fine fraction <60 μm). XRD analysis showed that clay fraction was mainly formed by kaolinite with illite and quartz (Table 1). It had a relatively average plasticity (Ip = 21) and high organic matter content (7.4%).

3.1.2. Infrared Spectroscopy. FTIR spectra of initial (before adsorption) AB and AP (Figure 2) showed characteristic bands of kaolinites (Table 2). Bands between 3620 cm^{-1} and 3700 cm^{-1} were characteristic of stretching vibrations of hydroxyl kaolinites [41]. Peaks were observed for OH-Al external bonds at 3670 cm^{-1} for AB and at 3652 cm^{-1} for AP and internal bonds at 3620 cm^{-1} [39, 42, 44]. The peak detected at 3652 cm^{-1} was assimilated to the hydroxyl bonds with the hydrogen of juxtaposed layers [45].

The peak observed at 3408 cm^{-1} on the AP spectrum was attributed to ferrous hydroxyls [39]. According to Saikia and

Table 1: Characteristics of raw Sejnane clay.

Elements	Yield
Kaolinite (%)	75.29
Illite (%)	9.87
Quartz(%)	14.84
CaO (%)	0.95
MgO (%)	1.18
SiO_2 (%)	56.33
Fe_2O_3 (%)	8.37
Al_2O_3 (%)	18.07
Na_2O (%)	0.14
K_2O (%)	1.38
SO_3 (%)	0.78
Fire waste	9.60

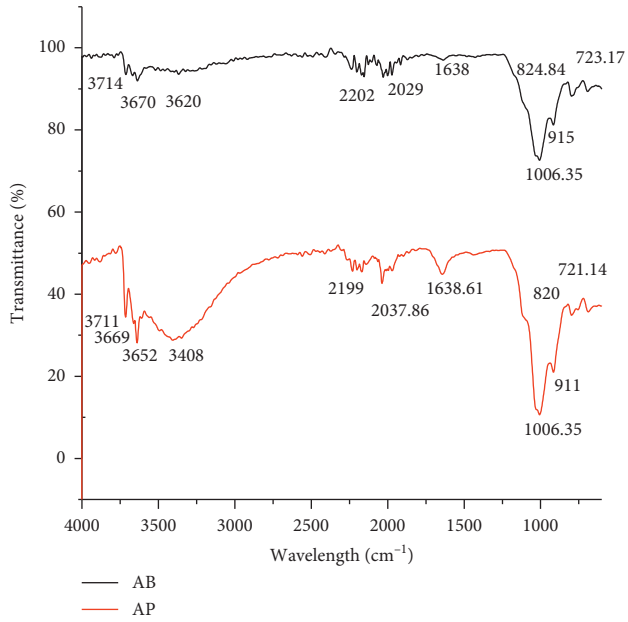

Figure 2: FTIR spectrum of raw (AB) and purified (AP) Sejnane clay.

Parasarathy [39], peaks observed between 1620 cm^{-1} and 1642 cm^{-1} were attributed to the flexion of H-OH bond. In the case of our clay, a band corresponding to this flexion appears at 1638 cm^{-1} on the spectra of crude and purified clay. FTIR spectra obtained were characterized by the appearance of several peaks between 400 cm^{-1} and 1200 cm^{-1}. Thus, peaks observed at 723 cm^{-1} on the AB spectrum and 721 cm^{-1} on the AP spectrum with an intense band at 1006 cm^{-1} corresponded to Si-O group elongation vibrations related to the presence of quartz [43, 45]. Presence of a shoulder at about 915 cm^{-1} is characteristic of internal Al-OH-Al bond deformation. These observations were in agreement with results of previous studies of kaolinites' infrared spectra in [44, 45]. OH stretching bands near 3620 cm^{-1} with the 751 cm^{-1} and 821 cm^{-1} bands certainly indicated the presence of illite. Bands appearing at 820 cm^{-1} and 824 cm^{-1} were characteristic of Fe-OH bonds [40].

3.1.3. SEM/EDX Analysis. Scanning electron microscopy had clearly shown the clay grains and leaflets lamellar structure. Aggregates of Sejnane clay were heterogeneous with different sizes and shapes and had rough surfaces. Thus, this material was porous, and the spaces between clay aggregates were well apparent (Figures 3 and 4).

Chemical microanalysis technique (EDS) used in conjunction with scanning electron microscopy (SEM) showed that major elements of Sejnane clay were oxygen (64%), silica (19%), and aluminum (8%) (Figures 5(a) and 5(b)).

Chemical microanalysis of clay grains surface (luminous and small crystals) (points 1, 2, 3, and 4 in Figure (5a)) showed no difference in chemical composition of all materials. It was probably free of silica crystals.

3.1.4. Physicochemical Characteristics of Raw and Activated Sejnane Clay. The average values of specific surface (SS), pH, electrical conductivity (EC), calcium carbonate ($CaCO_3$) rate, and cation-exchange capacity (CEC) of raw, purified, and activated clays that were used for adsorption tests are given in Table 3.

Maximum improvements of physicochemical values (SS and EC) were obtained with purified clay (AP) and activated clay with HCl. However, the maximum thermic activation (900°C) was accompanied with a small increase in SS (Table 3). The normality of activated solution that gave the best SS of activated clay is presented in Table 3 and used for the adsorption tests.

3.2. Adsorption Characteristics. The obtained results showed that purified Sejnane clay was a good adsorbate for reasons explained above. However, adsorption conditions of MG must be optimized to have a maximum performance. Parameters that were easily controlled were commonly evaluated such as the effect of initial dye concentration, solution/mass ratio of the clay, pH, and temperature. The results also determined the management mode and especially the degree of applicability of this technique at an industrial scale.

3.2.1. Effect of Contact Time, Initial Dye Concentration, and Clay Activation Procedure. Adsorption capacity of natural and purified Numidian clays was investigated with dye solution in the range from 30 mg·L^{-1} to 1 g·L^{-1}, with a clay mass of 0.5 g, at ambient temperature (about 25°C), and at constant pH. Samples were taken with 20 min time intervals.

To see if the AB or AP clays will allow elimination of maximum of MG quantities, we tested the adsorption capacities of raw clay activated in furnace (500–1100°C) and in chemical solutions (HCl and H_2SO_4) that had different temperature and normalities, respectively.

Figure 6 illustrates amounts of adsorbed dye per unit of clay increased with increasing initial concentration. MG removal from the aqueous phase to the AB and AP solid surface was fast during the first 5 minutes of the MG-clay contact. Then, the process was slowed down until reached its equilibrium. It was found that an extension of the contact time to 360 minutes did not lead to any changes in the amount of fixed dye for different concentrations studied. For AB, the speed of the phenomenon decreased with increase in

Table 2: FTIR spectra bands of raw (AB) and purified (AP) used clay.

Wavenumber (cm^{-1})		Assignments	References
AB	AP		
723	721	Si-O quartz	[39]
824	820	Fe-OH-Fe	[40]
915	915	Internal-surface OH bending	[41]
1006	1006	Si-O-Si symmetric stretch	[39, 42, 43]
1638	1638	H-O-H bending	[39, 43]
2029	2037	OH deformation of water	[39]
2202	2199	OH deformation of water	[39]
—	3408	Ferric hydroxyl	[39]
3620	—	Crystalline OH stretching	[39, 44, 45]
3670	3652	OH antisymmetric stretching (Al_2OH)	[39, 42]
3714	3711	OH stretching	[41]

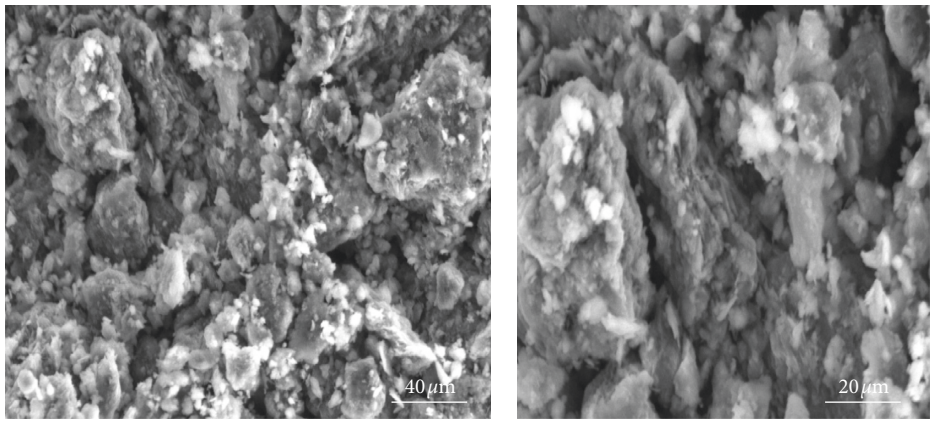

(a) (b)

Figure 3: View by scanning electron microscopy of raw clay (AB).

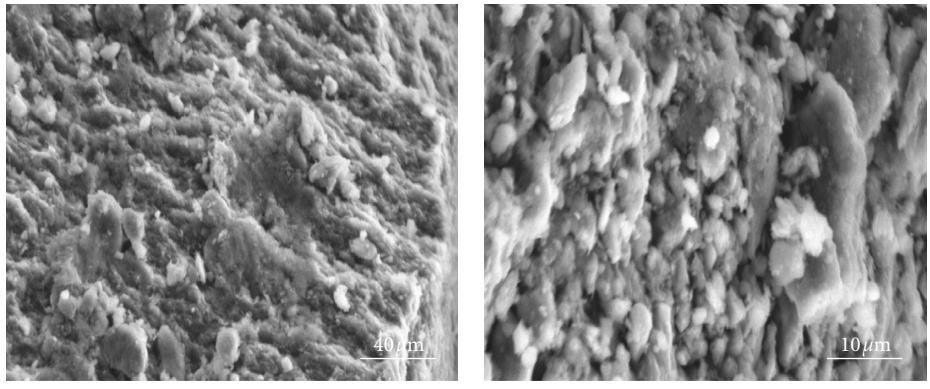

(a) (b)

Figure 4: View by scanning electron microscopy of purified clay (AP).

those concentrations. Discoloration reached its equilibrium towards the first 5 min for low concentrations; beyond 500 $mg{\cdot}L^{-1}$, the equilibrium time was extended to 80 min. This rapid saturation of clay for higher concentration was mainly due to the abundance and early availability of active sites of the clay surface. Similar results were mentioned in the previous study [46].

The presence of carbonates, organic matter, and associated minerals in the nontreated clays created a clutter on the adsorbent surface making it more difficult to access the MG cations at reactive sites, which prolonged the equilibrium time for AB.

Monitoring of discoloration yield for different MG concentrations showed that its value remained almost the same for different concentrations tested by AP. For AB adsorption, an increase in the dye content of 30 $mg{\cdot}L^{-1}$ to 1000 $mg{\cdot}L^{-1}$ was associated with a decrease in removal yield of approximately 26% (Figure 7). According to the obtained

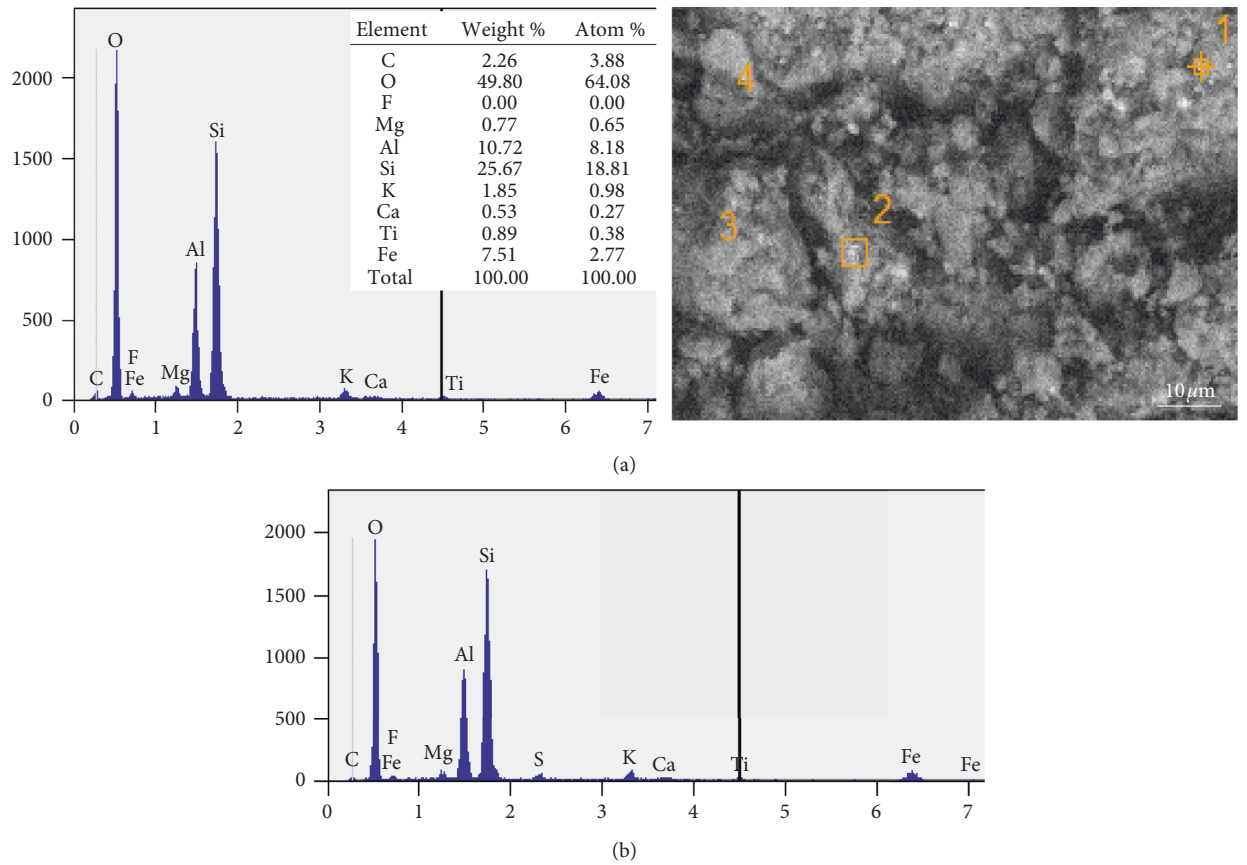

Figure 5: SEM image showing luminous crystals on raw clay (AB) surface (a) and energy-dispersive X-ray analysis (EDS) of point 2 (b).

Table 3: Statistic values of the maximum physicochemical parameters of raw and obtained clay by purification and activation of Sejnane clay type in different solution normalities and temperatures.

	pH	CE ($mScm^{-1}$)	$CaCO_3$ (%)	CEC (meq $100\,g^{-1}$)	SS ($m^2 \cdot g^{-1}$)
Raw clay	6.3 (5.9–6.5) ± 0.3*	0.37 (0.33–0.42) ± 0. 05*	4 (3.8–4.5) ± 0.4**	26.6 (25.9–27.5) ± 1.5*	37. 7 (35.5–40.1) ± 2.4***
HCl purification (0.1 N) and activation (0.5 N)	3.6 (3.3–3.9) ± 0.2*	3.4 (3.7–4.1) ± 0.3**	0	20 (18.9–22.5) ± 1.9**	168.5 (162.0–175.2) ± 13.1*
H_2SO_4 activation (3 N)	3.7 (3.6–3.9) ± 0.1**	1.9 (1.6–2.1) ± 0.2**	0	26.7 (24.9–29.8) ± 2.2***	116.2 (107.2–126.7.5) ± 10.1**
Thermic activation (900°C)	6.5 (6.2–6.7) ± 0.2***	3.5 (3.1–3.8) ± 0.3*	0.1 (0.7–1.6) ± 0.3***	20 (18.7–22.3) ± .1.9**	41.9 (37.1–49.1) ± 4.6*

Mean (minimum-maximum) ± standard deviation: * $p < 0.001$; ** $p < 0.015$; *** $p < 0.05$.

results, AP allowed for a better discoloration of up to 99.8% for an initial concentration of MG of 750 $mg \cdot L^{-1}$. Removal efficiency was important for fairly high dye concentrations and low adsorbent masses (0.5 (g)), thus demonstrating the effectiveness of the used material in the cationic dye removing. Since initial concentration of 750 $mg \cdot L^{-1}$ gave best performance of MG removal, the activated clays with 3 N H_2SO_4, 0.5 N HCl solutions, and high temperature (900°C thermal activation) were used for adsorption capacities tests (Figure 8).

Data presented in Figure 8 showed that best yields of MG elimination were with the clay purified with 0.1 N HCl and activated with 0.5 N HCl solutions. Thus, for what follows, only raw and purified clays will be considered.

3.2.2. Effect of Clay Mass. The parameter most commonly evaluated was the effect of solution/mass ratio of clay which was also easily controlled during the treatment of this type of wastewater. Solution of 100 ml of 750 $mg \cdot L^{-1}$ was used to test the effect of clay mass. Different doses (between 0.25 g and 3 g) of AP and AB were separately introduced at a fixed pH and temperature. Variations of percentages of MG retention as a function of clay mass were illustrated in Figure 9. We

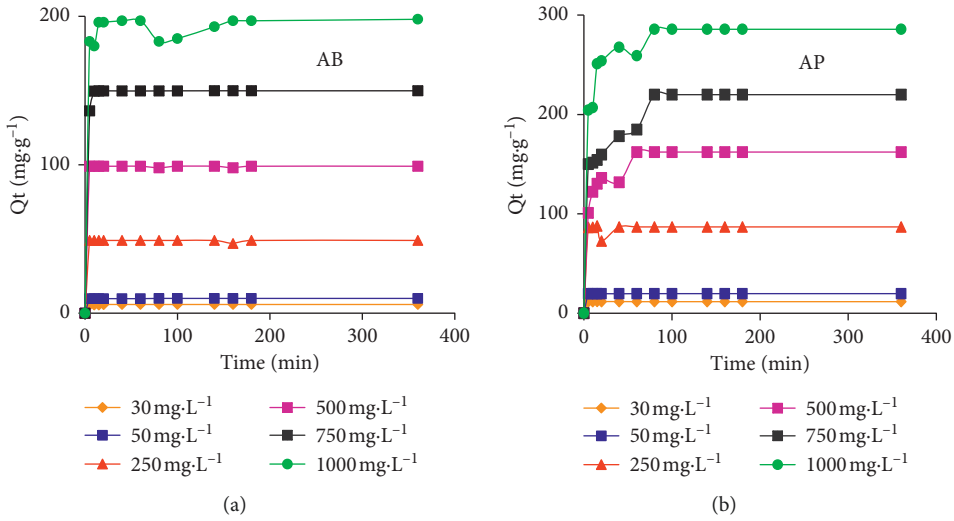

Figure 6: Influence of initial dye concentration variation on adsorption efficiency.

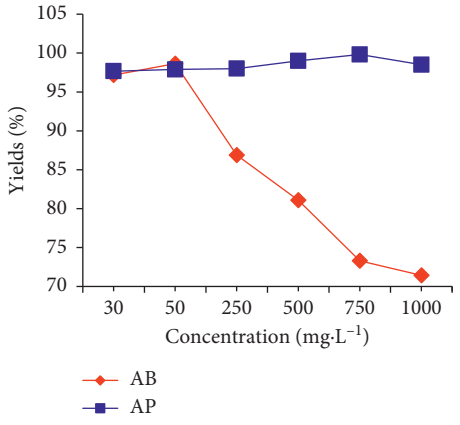

Figure 7: Variation of the adsorption yield according to the initial concentration of methyl green (MG).

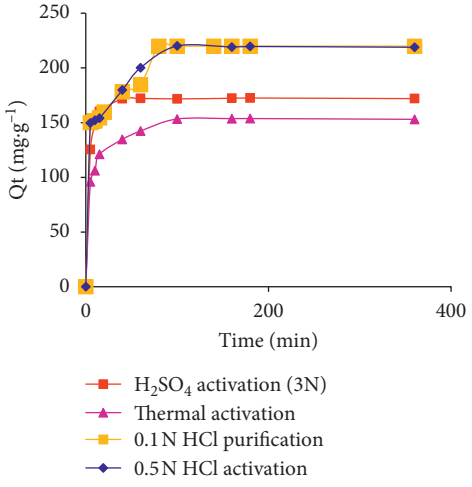

Figure 8: Adsorption capacities of clays activated with $T = 900°C$ and acid in the presence of an initial solution of 750 mg·L^{-1} MG. The adsorption capacity of HCl purified clay was kept as reference.

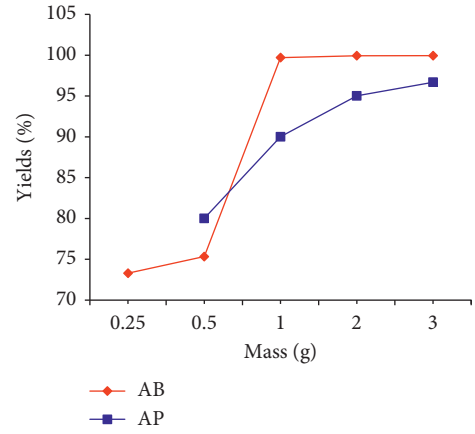

Figure 9: Influence of the variation of the mass of crude and purified Sejnane clay on the adsorption efficiency of methyl green.

noted that an increase in the adsorbent mass from 0.25 g to 2 g increased the discoloration degree from 73% to 99.9% for AB and from 80% to 95% for AP, to achieve the best efficiency. Thus, the number of adsorption sites was proportional to the adsorbent amount [13, 47].

3.2.3. Effect of pH and Temperature. The study of pH effect on dyes adsorption seems essential as it could affect the surface charge of adsorbent support and molecular structures of the adsorbate [1]. Discoloration of MG solutions was made at a pH ranging between 3 and 11 by AP and AB with a fixed clay mass and temperature. The obtained results are given in Figure 10.

The pH solution had no effect when MG was adsorbed on AP. For all tested pH, AP allowed adsorption of MG with rates greater than 99%. For AB clay, it was evident that acidification of the solution caused a significant drop in yield. MG adsorption increased with the increase in pH and reached its best yield (99.88%) at pH = 9. When the pH was

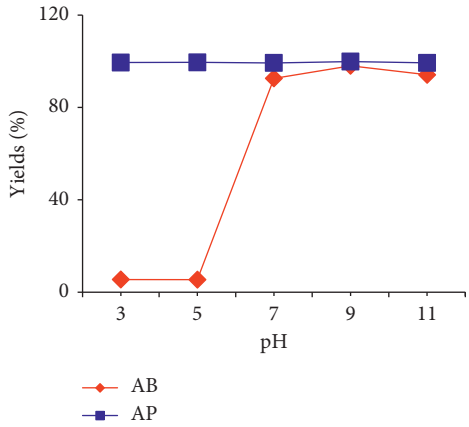

Figure 10: Influence of pH on the adsorption efficiency of methyl green by raw clay and purified Sejnane clay.

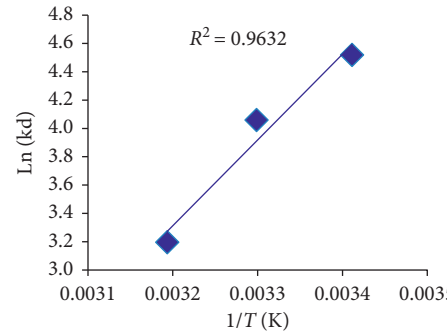

Figure 11: Effect of temperature on the distribution constant of the adsorption phenomenon.

equal to or greater than 7, its effect on adsorption became negligible. Thus, the increase in hydrogen ions created competition with dye cations for the active sites of clay surface [48, 49]. The same effect of pH was observed for basic textile dyes adsorption on natural clay [14]. However, for negatively charged dyes, the reverse effect was observed [22].

Effect of temperature on the adsorption processes is mentioned [50]. For our case, the effect of 20, 30, and 40°C that were commonly registered in arid and semiarid countries were tested. Dye concentration, AP and AB masses, and pH were fixed.

The tests showed that temperature was an influencing parameter for adsorption process of MG by Sejnane clay. Indeed, increasing temperature was directly related to the distribution coefficient of the dye between the two matrices (Figure 11). Therefore, the temperature advised was about 20°C because the increase in temperature made the pollutant elimination more difficult. The phenomenon was exothermic.

3.3. Adsorption Isotherms. The establishment of adsorption isotherms allowed us to determine the maximum retention capacity of the dye molecules and the adsorption type (Figure 12).

Equations (2) and (3) [41, 51], respectively, give linear forms of Langmuir and Freundlich isotherms:

$$\frac{\mathrm{Ce}}{\mathrm{Qe}} = \frac{1}{(\mathrm{Q\,max} * K_{\mathrm{L}})} + \frac{\mathrm{Ce}}{\mathrm{Q\,max}}, \quad (2)$$

$$\log(\mathrm{Qe}) = \frac{1}{n} \times \log(\mathrm{Ce}) + \log K_{\mathrm{F}}, \quad (3)$$

where K_{L} is the Langmuir constant, K_{F} is the Freundlich constant, and n is the energy constant of the digital distribution of sites.

Linearization of Langmuir and Freundlich equations (Figures 13(a) and 13(b)) allowed us to establish the characteristic parameters (Table 4). Experimental studies showed that the Langmuir model was not adequate to model the adsorption phenomenon of MG on AB and AP. However, the values of R^2 (0.97 for AB and AP) obtained from the Freundlich isotherm equation was higher than that from the Langmuir (0.96 for AB and 0.12 for AP) (Table 4). The Freundlich model could describe well the studied process. Therefore, the adsorption of this dye was not in monolayer occurring on homogeneous sites [14]; each site was able to capture more than one cation, the dye cations had interaction between them [52], and the adsorption was not reversible. Thus, it was chemisorption where we had a multilayer adsorption on a heterogeneous surface, and when the adsorption capacity increased, other new adsorption sites appeared.

The values of n and $1/n$ which gave an idea about the adsorption intensity or the heterogeneity or nondistribution of molecules on the adsorbent surface [52] were calculated for AB and AP. For AB, the n value close to 0 showed that the adsorption surface was more heterogeneous [53], and the ratio $1/n = 0.363 < 0.7$ implied that isotherms of MG were strongly curved (European Centre for Ecotoxicology and Toxicology of Chemicals). For AP, n value was equal to 0.859 and the ratio was $1/n$ greater than 1 implying that isotherms were of type S according to Giles classification (European Centre for Ecotoxicology and Toxicology of Chemicals). KF value, which gave information on the adsorption capacity, was higher for AP. Thus, the adsorption capacity of AP was greater than that of nontreated clay [54].

3.4. Kinetics of Adsorption. To study the order of the adsorption reaction and to correlate the experimental results with each other, pseudo-first-order models, pseudo-second-order models, and intraparticle diffusion models were applied for a clay mass of 0.5 g and a solution of MG with a concentration of 750 mg·L^{-1}.

The plots of the adsorbed amount of MG (mg·g^{-1}) versus contact time are given in Figure 14 where Qt vs. time was plotted for both kinetic models [55]. Kinetics of adsorption of MG by Sejnane clay showed that the colorant uptake increased with contact time for AB, while it decreased with time for AP until they reached the equilibrium state within 10 and 240 minutes for AB and AP, respectively.

The use of kinetic models helps understanding of the adsorption mechanism of methyl green by Sejnane clay. Pseudo-first-order and pseudo-second-order models are shown in the following equations [56, 57], respectively:

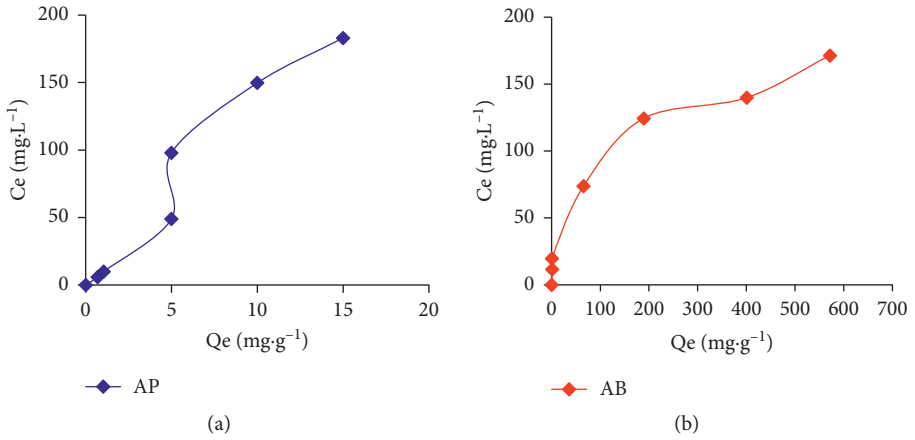

Figure 12: Adsorption isotherms of AP (a) and AB (b).

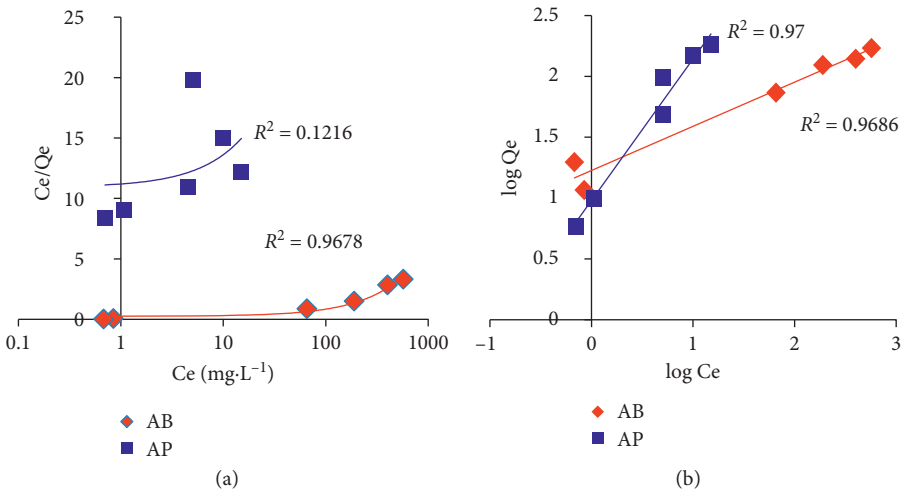

Figure 13: Adsorption isotherms according to Langmuir (a) and (b) Freundlich models of purified and crude clays.

Table 4: Characteristic parameters of the Langmuir and Freundlich isotherms.

	Langmuir			Freundlich		
	Qmax (mg·g^{-1})	K_L	R^2	K_F	$1/n$	R^2
AB	169.49	0.02328	0.96	3.41	0.36	0.97
AP	175.44	0.00057	0.12	9.55	1.16	0.97

AB: raw clay; AP: purified clay.

$$\frac{d\mathrm{Qt}}{dt} = k_L(\mathrm{Qe} - \mathrm{Qt}), \quad (4)$$

$$\frac{d\mathrm{Qt}}{dt} = k_B(\mathrm{Qe} - \mathrm{Qt})^2, \quad (5)$$

where Qe is the quantity of the adsorbate at equilibrium (mg·g^{-1}); t is the contact time (min); k_L is the Lagergren constant, adsorption rate constant for the first order (min^{-1}); and k_B is the Blanchard constant, adsorption rate constant for the pseudo-second order (g·mol^{-1}·min^{-1}). Equations (4) and (5) were converted to the linear form given in equations (6) and (7), respectively, for pseudo-first and pseudo-second orders. Linear plots are illustrated in Figure 14.

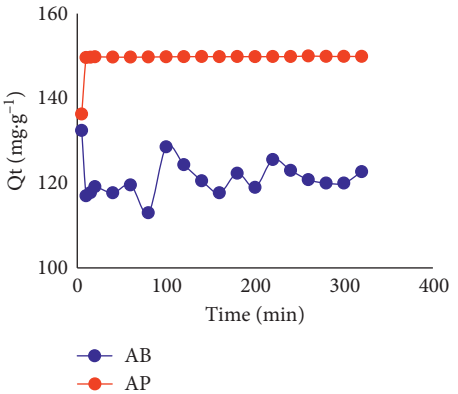

Figure 14: Adsorption kinetics of MG by Sejnane clay.

$$\mathrm{Ln}\,(\mathrm{Qe}-\mathrm{Qt}) = -k_{\mathrm{L}} \times t + \ln \mathrm{Qe}, \tag{6}$$

$$\frac{t}{\mathrm{Qt}} = \frac{1}{k_{\mathrm{B}} \times \mathrm{Qe}^2} + \frac{t}{\mathrm{Qe}}. \tag{7}$$

The Lagergren model characterizes the adsorption rate according to adsorption capacity. It is assumed that the rate of retention was proportional to Qe − Qt and the phenomenon was reversible [57]. The best kinetic plot using the proposed equation was of the pseudo-second-order kinetic model (Figure 15). This plot was close to linearity and gave good regression coefficient (R^2) with a range of 0.999 for AB and AP, respectively. The calculated parameters considering that the plot was linear are listed in Table 5.

The pseudo-second-order model described adsorption depending on available sites by taking into account both rapid and slow fixation of dye molecules at the most reactive clay sites as well as low-energy sites [55]. This model suggested a chemisorption resulting from an electron exchange between the dye cations and the functional groups of the adsorbent [58]. The application of the intraparticle diffusion model made it possible to obtain the results illustrated in Figure 16. The curves obtained were derived from the linearization of the adsorbed quantities Qt ($\mathrm{mg{\cdot}g^{-1}}$) as a function of $t^{1/2}$ ($\mathrm{min}^{1/2}$) and are described by the following relation [11]:

$$\mathrm{Qt} = k_{\mathrm{p}} t^{1/2} + C, \tag{8}$$

where C is the intercept and k_{p} is the intraluminal scattering constant ($\mathrm{mg{\cdot}g^{-1}\,min^{1/2}}$).

The graphical representation of the straight lines resulting from the relations described by using equations (6)–(8) (Figures 15 and 16) and the theoretical values determined (Table 5) showed that the pseudo-second-order model was better fit to describe the kinetics of methyl green adsorption on AB and AP with correlation coefficients of 0.999. The quantities of the adsorbed dye at equilibrium calculated by this model were very close to those determined experimentally. In our case, we could therefore adopt the hypothesis of chemisorption carried out by electron exchange on the surface of the clays used. These data confirmed the results deduced from the adsorption isotherms.

Several previous studies on the adsorption of dyes on clay adsorbents also showed that this phenomenon obeyed the pseudo-second-order [17, 59, 60]. Adsorption rate constants (K_{b}) were $0.044\,\mathrm{g{\cdot}mg^{-1}\ min^{-1}}$ for AB and $0.0335\,\mathrm{g{\cdot}mg^{-1}\ min^{-1}}$ for AP, testifying a significant attraction speed of the coloring molecules by natural clay. Similar results were observed for the adsorption of MG on graphene sheets [11].

3.5. Adsorption Thermodynamic Parameters and Mechanism. Since all results indicated that purified clay was better indicated for MG removal, thermodynamic parameters were calculated only for AP.

The results indicated that the temperature increase allowed improvements in Ln values of the distribution constant (Figure 11).

From the slope and intercept of the log trend curve K_{d} versus $1/T$ obtained from the following relations [61]:

$$\mathrm{Ln}\,K_{\mathrm{d}} = \frac{\Delta S^{\circ}}{R} - \frac{\Delta H^{\circ}}{\mathrm{RT}}, \qquad K_{\mathrm{d}} = \frac{\mathrm{Qe}}{\mathrm{Ce}}, \tag{9}$$

where K_{d} is the distribution constant; R is the constant of perfect gases ($\mathrm{J{\cdot}mol^{-1}{\cdot}K^{-1}}$); T is the absolute temperature (K); ΔS is the entropy standard ($\mathrm{kJ{\cdot}mol^{-1}{\cdot}K^{-1}}$); and ΔH is the enthalpy Standard.

The standard free enthalpy ΔG° was calculated using equation (10):

$$\Delta G = -\mathrm{RT} \ln K_{\mathrm{d}}. \tag{10}$$

The enthalpy and the entropy values of the adsorption were calculated (Table 6). ΔH° values were greater then $40\,\mathrm{J{\cdot}k{\cdot}mol^{-1}}$ (Table 6), confirming that the adsorption was endothermic and of chemisorption type [62]. Negative values of ΔG° which increased with the solution temperatures allowed us to conclude that the dye adsorption on Sejnane clay was spontaneous [10] and that the increase in temperature hindered the dye elimination [63]. Therefore, we confirmed that ambient temperature is advised to reach better yields of MG removal.

3.6. Sejnane Clay Efficiency. This efficiency was further confirmed by comparing the experimental results of the present work with those obtained in previous studies (Table 7). The comparison concerned either the elimination of the same dye by adsorption on other adsorbent supports, or with its treatment with biological or photochemical processes. In fact, Sejnane clay, by virtue of these surface characteristics and its high cation retention capacity, had discoloration rates (water that was fairly concentrated in MG) much larger than methods given in Table 7.

3.7. Clay Characterization after Adsorption

3.7.1. FTIR Analysis. Comparison of FTIR spectra of the used purified clay before and after adsorption showed appearance of additional peaks after their contact with the MG dye (Figure 17). Peaks appearing at 1359 and 1496 were characteristics of C-H bonds, at 2005 were characteristics of the -C═C bonds, and at 3533 were of the O-H bonds. A comparison between newly appeared peaks with those of MG showed that the new peaks were probably the characteristic of this textile pollutant. This information testified the intercalation of the dye on the clay molecules. This proposition was confirmed by a slight increase in the 634 peak intensity that corresponded to the specific position of the Si-O-Si bonds, reflecting the existence of C═C-H hydrogen bonds between the dye and the clay. We also noted displacement of the peak of the H-O-H bond located at 1641 to the position 1610 with an increase in its width following the hydrogen bonding with the N atom of MG (N-H bond).

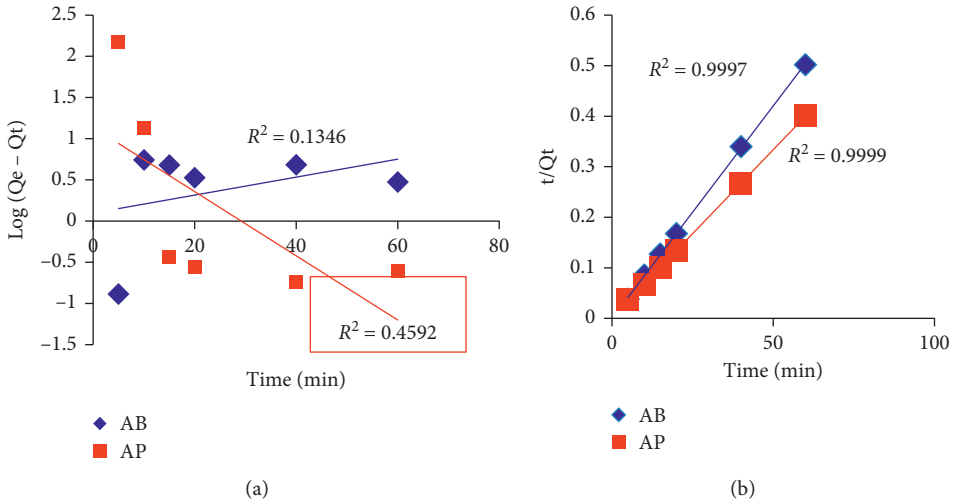

Figure 15: Application of the Lagergren (a) and Blanchard (b) models for the adsorption of methyl green by Sejnane clay.

Table 5: Kinetic parameters of adsorption of methyl green on Sejnane Clay.

Clay	Qe_{exp} (g·mg^{-1})	Pseudo-first-order			Pseudo-second-order			Intraparticular diffusion		
		K_L (min^{-1})	Qe (g·mg^{-1})	R^2	K_b (g·mg^{-1} min^{-1})	Qe (g·mg^{-1})	R^2	K_p	C	R^2
AB	119.6	0.003	3.93	0.13	0.04	119.04	0.99	2.78	88.9	0.19
AP	149.9	0.150	66.47	0.46	0.03	151.51	0.99	3.70	107,6	0.23

AB: raw clay; AP: purified clay.

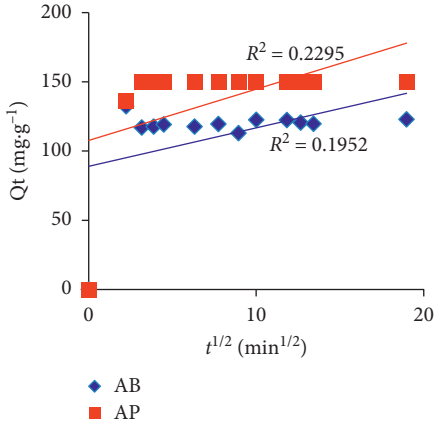

Figure 16: Kinetic model of intraparticular diffusion.

Table 6: Thermodynamic parameters of adsorption of methyl green on purified clay.

T (K°)	AP				
	Yield (%)	$\Delta H°$ (kJ·mol^{-1})	$\Delta S°$ (kJ·mol^{-1}·K^{-1})	R^2	$\Delta G°$ (kJ·mol^{-1})
293.15	99.77				−11016.0
303.15	86.70	50339.6	−133.5	0.96	−10231.2
313.15	86.88				−8320.4

AP: purified clay.

Comparison of MG infrared spectra and AB before and after adsorption showed also some modifications (Figure 17). For the saturated raw clay with MG, an addition of peaks characterizing the C-H groups (1237 and 3004) of MG was detected. This variation of C-H bonds of the clay mineral substrate was due to the increase in intensity of characteristic

Table 7: Removal of green methyl (MG) using different materials and processes.

Processing	Initial concentrations of MG ($mg{\cdot}L^{-1}$)	Yield (%)	Reference
Adsorption on kaolinic AB from Sejnane	750	73.3	This work
Adsorption on kaolinic AP from Sejnane	750	99.8	This work
Adsorption on activated carbon	30	80	[10]
Adsorption on graphene sheet	100	71.5	[11]
Adsorption on activated bentonite	20	70.7	[12]
Photodecolorization on synthetic zeolite	40	80	[6]
Biodegradation by *Staphylococcus epidermidis*	750	80	[9]
UV direct photolysis	25	66	[8]
Photolysis by H_2O_2/UV	25	86	[8]
Photolysis by acetone/UV	25	100	[8]

AB: raw clay; AP: purified clay.

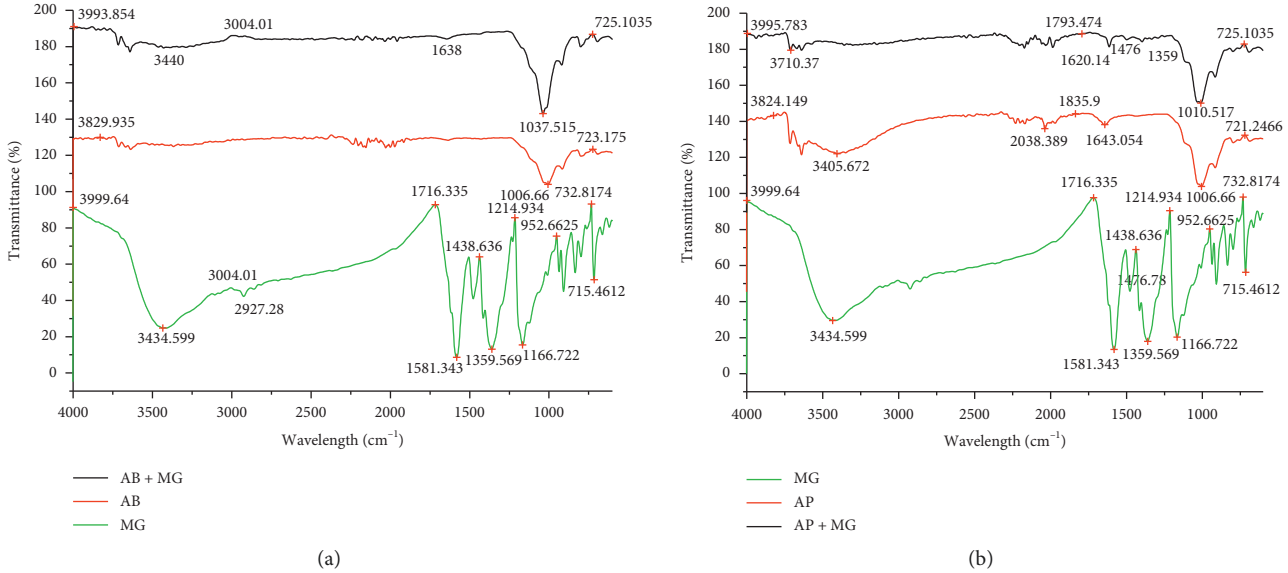

Figure 17: FTIR spectrum of MG and clays used before and after adsorption.

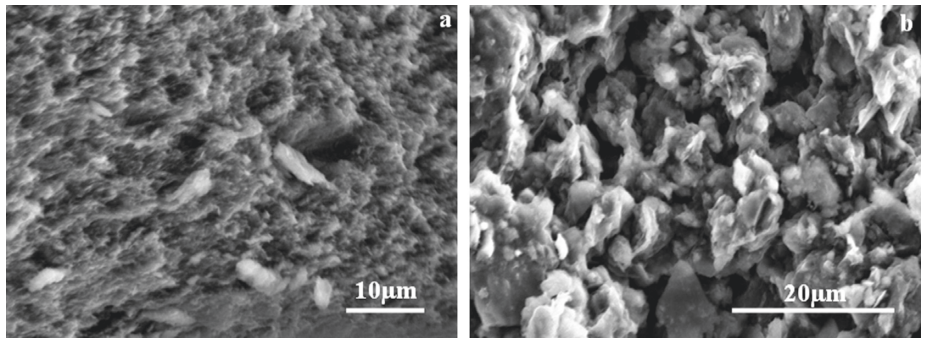

Figure 18: Scanning electron microscopy view of raw clay (a) and purified clay (b) after MG adsorption.

bands of O-H groups (peak 1151). An increase in the intensity of peaks 1037 and 1006 which were specific to Si-O bonds was also noted. This increase was probably due to the oxygen-hydrogen bonds that the dye established with the adsorbent. Similarly, an increase in peaks intensity specific to Al-O-H bonds (peaks 3640 and 3694) was remarked. These modifications were also observed in X-ray diffraction diagrams [6, 64].

3.7.2. SEM/EDX Analysis. Scanning electron microscopy showed a remarkable change in the surface morphology after adsorption (Figure 18). Indeed, a noticeable decrease in the porosity and the roughness of adsorbent surface was observed. There were also certain homogenizations of the surface following recovery of clay grains by MG cations.

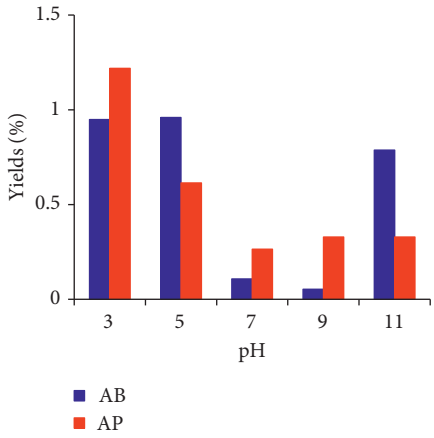

Figure 19: Desorption yields of methyl green at different pH values.

3.8. Desorption Test. The study of MG desorption from natural clays (Figure 19) showed that less than 1.5% of the dye was desorbed for an acidic or strongly basic pH (pH = 11) and less than 0.5% when the pH was between 7 and 9 (the most frequent pH of wastewater). Thus, retention binding energies of these pollutants were high, and hence, MG adsorbed by Sejnane clays posed many environmental problems.

4. Conclusion

The major constituent of the heterogeneous clay type that was sampled from the Sejnane site is the kaolinite. This geological material contains a small quantity of illite. However, smectite that had a high adsorption capacity is totally absent. Thus, this heterogeneous material can have a low performance of dye elimination per volume unit. Kaolinitic clay was always considered as a good anionic dye adsorbent. In this study, the adsorptive capacity of cationic dyes by kaolinite clay was tested. The speed and the capacity of cationic methyl green removals with nontreated and purified natural Sejnane clay were tested. To optimize the adsorption conditions of MG on Sejnane clays, effects of initial dye concentration, contact time, clay mass per unit volume, pH, temperature, and acid and thermic activation were studied.

Obtained results showed that Sejnane clay type had an important retention capacity of the cationic dye. With an initial solution of 750 $mg{\cdot}L^{-1}$ at pH = 9, the maximum of dye quantity was fast adsorbed with 0.5 g of clay. The purified clay with 0.1 N HCl and activated with 0.5 NaCl had a higher yield (99.8%) than of the raw clay (73.3%) and of activated clay with H_2SO_4 and high temperature (900°C). Only the photolysis by acetone/UV had eliminated the total MG quantities. Taking into account the cost of this treatment and the complexity of the photolysis process, Sejnane clay-kaolinite type remains the most profitable.

Obtained results showed that the pH range 7–11 and the ambient temperature of polluted water were the best condition to have highest elimination of MG dye quantities. These results had shown moreover the effectiveness of kaolinitic clay in cationic dye removal.

To better understand how the dye cations were fixed by molecules of the material tested, adsorption isotherms and kinetic study were performed and thermodynamic parameters were calculated. Results indicated that adsorption of MG on nontreated and purified Sejnane clay followed the pseudo-second order. Equilibrium states were described by Freundlich isotherm. We therefore had a chemisorption that occurred on a multilayer heterogeneous surface (clay dye) with electron exchange between clay and dye. Calculated thermodynamic parameters specified that this process was spontaneous and endothermic. Comparison of clays' FTIR spectra before and after adsorption confirmed that the summed peaks were of MG.

Scanning electron microscopy (SEM) and chemical microanalysis technique (EDS) showed that Sejnane clay had homogeneous composition and the adsorbed MG induced remarkable changes in surface morphology of the used clay. This adsorption was achieved through high-energy bonds since only a very small amount of MG could be desorbed. Hence, the products used do not pose any environmental risks.

Data Availability

The data used to support the findings of this study are available from the corresponding author upon request.

Conflicts of Interest

The authors declare that they have no conflicts of interest.

Acknowledgments

The authors would like to thank Pr. Simon Sheppared for the English language revision. This study was financially supported by the Tunisian Ministry of High and Education and Scientific Researches.

References

[1] M. Laabd, E. Abdelhadi, C. Hafsa, A. Nouh, M. Bazzaoui, and A. Albourine, "Etude cinétique et thermodynamique de l'adsorption des colorants monoazoïques sur la polyaniline," *Journal of Materials and Environnemental Science*, vol. 6, no. 4, pp. 1049–1059, 2015.

[2] T. Sauer, G. Cesconeto Neto, H. J. José, and R. F. P. M. Moreira, "Kinetics of photocatalytic degradation of reactive dyes in a TiO_2 slurry reactor," *Journal of Photochemistry and Photobiology A: Chemistry*, vol. 149, no. 1–3, pp. 147–154, 2002.

[3] John Wiley & Sons, *Ullmann's Encyclopedia of Industrial Chemistry*, vol. 27, John Wiley & Sons, Hoboken, NJ, USA, 2001.

[4] B. G. Berg and D. M. Green, "Spectral weights in profile listening," *The Journal of the Acoustical Society of America*, vol. 88, no. 2, pp. 758–766, 1990.

[5] T. Geethakrishnan and P. K. Palanisamy, "Degenerate four-wave mixing experiments in methyl green dye-doped gelatin film," *Optik*, vol. 117, no. 6, pp. 282–286, 2006.

[6] A. Nezamzadeh-Ejhieh and E. Shahriari, "Heterogeneous photodecolorization of methyl green catalyzed by Fe(II)-o-phenanthroline/zeolite Y nanocluster," *International Journal of Photoenergy*, vol. 2011, Article ID 518153, 10 pages, 2011.

[7] A. Nezamzadeh-Ejhieh and K. Shirvani, "CdS loaded an Iranian clinoptilolite as a heterogeneous catalyst in photodegradation of *p*-aminophenol," *Journal of Chemistry*, vol. 2013, Article ID 541736, 11 pages, 2013.

[8] I. Bousnoubra, K. Djebbar, A. Abdessemed, and T. Sehili, "Decolorization of methyl green and bromocresol purple in mono and binary systems by photochemical processes: direct UV photolysis, acetone/UV and H2O2/UV: a comparative study," *Desalination and Water Treatment*, vol. 57, pp. 1–16, 2016.

[9] L. Ayed, K. Chaieb, A. Cheref, and A. Bakhrouf, "Biodegradation and decolorization of triphenylmethane dyes by Staphylococcus epidermidis," *Desalination*, vol. 260, no. 1–3, pp. 137–146, 2010.

[10] O. Baghriche, K. Djebbar, and T. Sehili, "Etude cinétique de l'adsorption d'un colorant cationique (vert de methyle) sur du charbon actif en milieu aqueux," *Science Technologies*, vol. 27, pp. 57–62, 2008.

[11] A. A. Farghali, M. Bahgat, W. M. A. El Rouby, and M. H. Khedr, "Preparation, decoration and characterization of graphene sheets for methyl green adsorption," *Journal of Alloys and Compounds*, vol. 555, pp. 193–200, 2013.

[12] A. Maghni, M. Ghelamallah, and A. Benghalem, "Sorptive removal of methyl green from aqueous solutions using activated bentonite," *Acta Physica Polonica A*, vol. 132, no. 3, pp. 448–450, 2017.

[13] W.-T. Tsai, H.-C. Hsu, T.-Y. Su, K.-Y. Lin, C.-M. Lin, and T.-H. Dai, "The adsorption of cationic dye from aqueous solution onto acid-activated andesite," *Journal of Hazardous Materials*, vol. 147, no. 3, pp. 1056–1062, 2007.

[14] A. B. Karim, B. Mounir, M. Hachkar, M. Bakasse, and A. Yaacoubi, "Élimination du colorant basique « bleu de méthylène » en solution aqueuse par l'argile de Safi," *Revue des Sciences De l'Eau*, vol. 23, no. 4, pp. 375–388, 2010.

[15] N. Hamouda, I. Zouari, A. Gannouni, and A. Bellagi, "Elimination d'un colorant des rejets de l'industrie textile par la technique d'adsorption sur une argile naturelle dans un lit fluidisé," *Journal de la Société de Chimie Tunisie*, vol. 9, pp. 29–39, 2007.

[16] S. Guiza, K. Ghiloufi, and F. M. Bagane, "Utilization of waste Tunisian palm tree date as low-cost adsorbent for the removal of dyes from textile wastewater," *Mediterranean Journal of Chemistry*, vol. 3, no. 5, pp. 1044–1052, 2014.

[17] B. Benguella and A. Yacouta-Nour, "Elimination des colorants acides en solution aqueuse par la bentonite et le kaolin," *Comptes Rendus Chimie*, vol. 12, no. 6-7, pp. 762–771, 2009.

[18] S. T. Akar and R. Uysal, "Untreated clay with high adsorption capacity for effective removal of C.I. acid red 88 from aqueous solutions: batch and dynamic flow mode studies," *Chemical Engineering Journal*, vol. 162, no. 2, pp. 591–598, 2010.

[19] W. Luo, K. Sasaki, and T. Hirajima, "Influence of the predispersion of montmorillonite on organic modification and the adsorption of perchlorate and methyl red anions," *Applied Clay Science*, vol. 154, pp. 1–9, 2018.

[20] N. Abidi, J. Duplay, A. Jada et al., "Toward the understanding of the treatment of textile industries' effluents by clay: adsorption of anionic dye on kaolinite," *Arabian Journal of Geoscience*, vol. 10, no. 16, p. 373, 2017.

[21] M. Bagane and S. Guiza, "Elimination d'un colorant des effluents de l'industrie textile par adsorption," *Annales de Chimie Science des Matériaux*, vol. 25, no. 8, pp. 615–625, 2000.

[22] E. Errais, J. Duplay, F. Darragi et al., "Efficient anionic dye adsorption on natural untreated clay: kinetic study and thermodynamic parameters," *Desalination*, vol. 275, no. 1–3, pp. 74–81, 2011.

[23] I. Chaâri, K. Jridi, E. Fakhfakh, F. Jamoussi, and A. Mnif, "Use of Tunisian raw clay to remove dye from aqueous solution," *Arabian Journal of Geoscience*, vol. 9, no. 10, p. 564, 2016.

[24] S. Ghrab, S. Mefteh, M. Medhioub, and M. Benzina, "Adsorption of nickel(II) and chromium(III) from aqueous phases on raw smectite: kinetic and thermodynamic studies," *Arabian Journal of Geoscience*, vol. 11, no. 16, p. 440, 2018.

[25] L. Khalfa, M. L. Cervera, M. Bagane, and S. Souissi-Najar, "Modeling of equilibrium isotherms and kinetic studies of Cr (VI) adsorption into natural and acid-activated clays," *Arabian Journal of Geosciences*, vol. 9, no. 1, 2016.

[26] P. Gregory, "Dyes and dyes intermediates," in *Encyclopedia of Chemical Technology*, J. I. Kroschwitz, Ed., vol. 8, pp. 544-545, John Wiley & Sons, New York, NY, USA, 1993.

[27] H. Rouvier, "Géologie de l'extrême-nord Tunisien: tectoniques et paléogéographies superposées à l'extrémité orientale de la chaîne nord maghrébine," Thèse d'Etat, Université Paris-6, Paris, France, 1977.

[28] C. Yaich, H.-J.-F. Hooyberghs, C. Durlet, and M. Renard, "Corrélation stratigraphique entre les unités oligo-miocènes de Tunisie centrale et le Numidien," *Comptes Rendus de l'Académie des Sciences—Series IIA-Earth and Planetary Science*, vol. 331, no. 7, pp. 499–506, 2000.

[29] L. G. Schultz, *Quantitative Interpretation of Mineral Composition from X-Ray and Chemical Data for the Pierre Shale US Geol. Survey*, United States Government Printing Office, Washington, DC, USA, 1964.

[30] H. W. Van der Marel, "Quantitative analysis of clay minerals and their admixtures," *Contributions to Mineralogy and Petrology*, vol. 12, no. 1, pp. 96–138, 1966.

[31] A. Lopez Galindo, J. Torres Ruiz, and J. M. Gonzalez Lopez, "Mineral quantification in sepiolite-palygorskite deposits using X-ray diffraction and chemical data," *Clay Minerals*, vol. 31, no. 2, pp. 217–224, 1996.

[32] J. Beaulieu, "Identification géochimique de matériaux argileux naturels par la mesure de leur Surface au moyen du bleu de méthylène," Thèse Université, Orsay, Paris, France, 1979.

[33] G. W. Phelps and D. L. Harris, "Specific surface and dry strength by methylene blue adsorption," *American Ceramic Society Bulletin*, vol. 47, no. 12, pp. 1146–1150, 1967.

[34] LCPC, *Limite d'Atterberg-Limite de Liquidité-Limite de Plasticité Méthode d'Essai*, LCPC, Rochester, NY, USA, 1987.

[35] B. Muhunthan, "Discussion of influence of changes in methanol concentration on clay particle interactions," *Canadian Geotechnical Journal*, vol. 21, pp. 266-267, 1990.

[36] Mineralogical Association of Canada, *Infrared Spectroscopy in Geochemistry, Exploration Geochemistry, and Remote Sensing*, P. L. King, M. S. Ramsey, and G. A. Swayze, Eds., Mineralogical Association of Canada, Quebec City, Canada, 2004.

[37] M. Suziki, *Adsorption Engineering*, Elsevier, New York, USA, 1990.

[38] I. Langmuir, "The adsorption of gases on plane surfaces of glass, mica and platinum," *Journal of the American Chemical Society*, vol. 40, no. 9, pp. 1361–1403, 1918.

[39] J. B. Saikia and G. Parasarathy, "Fourier transforms infrared spectroscopic characterization of kaolinite from Assam and Meghalaya, north eastern India," *Journal Modern Physics*, vol. 1, no. 4, pp. 206–210, 2010.

[40] J. Madejová, J. Kečkéš, H. Pálková, and P. Komadel, "Identification of components in smectite/kaolinite mixtures," *Clay Minerals*, vol. 37, no. 2, pp. 377–388, 2002.

[41] V. C. Farmer, "Infrared spectroscopy in clay mineral studies," *Clay Minerals*, vol. 7, no. 4, pp. 373–387, 1968.

[42] M. A. Qtaitat and I. N. Al-Trawneh, "Characterization of kaolinite of the Baten El-Ghoul region/south Jordan by infrared spectroscopy," *Spectrochimica Acta Part A: Molecular and Biomolecular Spectroscopy*, vol. 61, no. 7, pp. 1519–1523, 2005.

[43] A. Moufti, "Étude physico-chimique des eaux d'exhaure de Youssoufia (Maroc) et leur défluoruration par adsorption sur la cellulose et les cendres volantes à charbon," Thèse Doct, Univ. Chouaib Doukkali, Faculté des Sciences, El Jadida, Marocco, 2003.

[44] V. C. Farmer and J. D. Russell, "The infra-red spectra of layer silicates," *Spectrochimica Acta*, vol. 20, no. 7, pp. 1149–1173, 1964.

[45] J. Madejová, "FTIR techniques in clay mineral studies," *Vibrational Spectroscopy*, vol. 31, no. 1, pp. 1–10, 2003.

[46] M. El Alouani, S. Alehyen, M. El Achouri, and M. Taibi, "Preparation, characterization, and application of Metakaolin-based geopolymer for removal of methylene blue from aqueous solution," *Journal of Chemistry*, vol. 2019, Article ID 4212901, 14 pages, 2019.

[47] V. K. Gupta, A. Mittal, and V. Gajbe, "Adsorption and desorption studies of a water soluble dye, Quinoline Yellow, using waste materials," *Journal of Colloid and Interface Science*, vol. 284, no. 1, pp. 89–98, 2005.

[48] Y. Fu and T. Viraraghavan, "Removal of congo red from an aqueous solution by fungus Aspergillus niger," *Advances in Environmental Research*, vol. 7, no. 1, pp. 239–247, 2002.

[49] S. V. Mohan, N. C. Raoet, and J. Karthikeyan, "Adsorptive removal of direct azo dye from aqueous phase onto coal based sorbents: a kinetic and mechanistic study," *Journal of Hazardous Materials*, vol. 90, no. 2, pp. 189–204, 2002.

[50] Z. Al-Qodah, "Adsorption of dyes using shale oil ash," *Water Research*, vol. 34, no. 17, pp. 4295–4303, 2000.

[51] H. M. F. Freundlich, "Over the adsorption in solution," *Journal of Physical Chemistry*, vol. 57, pp. 385–470, 1906.

[52] L. Sala, F. S. Figueira, G. P. Cerveira, C. C. Moraes, and S. J. Kalil, "Kinetics and adsorption isotherm of C-phycocyanin from spirulinaplatensis on ion-exchange resins," *Brazilian Journal of Chemical Engineering*, vol. 31, no. 4, pp. 6604–6632, 2014.

[53] F. Haghseresht and G. Q. Lu, "Adsorption characteristics of phenolic compounds onto coal-reject-derived adsorbents," *Energy & Fuels*, vol. 12, no. 6, pp. 1100–1107, 1998.

[54] J. C. Igwe and A. A. Abia, "A bioseparation process for removing heavy metals from waste water using biosorbents," *African Journal of Biotechnology*, vol. 5, pp. 1167–1179, 2006.

[55] A. Aarfane, A. Salhi, M. El Krati et al., "Etude cinétique et thermodynamique de l'adsorption des colorants Red195 et bleu de méthylène en milieu aqueux sur les cendres volantes et les mâchefers," *Journal of Materials and Environnemental Science*, vol. 5, pp. 1927–1939, 2014.

[56] S. Lagergren, "About the theory of so-called adsorption of soluble substances," *Kungliga Svenska Vetenskapsakademiens Handlingar*, vol. 24, pp. 1–39, 1898.

[57] G. Blanchard, M. Maunaye, and G. Martin, "Removal of heavy metals from waters by means of natural zeolites," *Water Research*, vol. 18, no. 12, pp. 1501–1507, 1984.

[58] R. Cavet, *Le sol—Propriétés et Fonction*, Tome 1: Edition France Agricole, Paris, France, 2003.

[59] Y. S. Ho and G. Mckay, "Pseudo-second order model for sorption processes," *Process Biochemistry*, vol. 34, no. 5, pp. 451–465, 1999.

[60] S. Wang, Y. Boyjoo, A. Choueib, and Z. H. Zhu, "Removal of dyes from aqueous solution using fly ash and red mud," *Water Research*, vol. 39, no. 1, pp. 129–138, 2005.

[61] J. Yener, T. Kopac, G. Dogu, and T. Dogu, "Adsorption of basic yellow 28 from aqueous solutions with clinoptilolite and amberlite," *Journal of Colloid and Interface Science*, vol. 294, no. 2, pp. 255–264, 2006.

[62] Z. Bouberka, S. Kacha, M. Kameche, S. Elmaleh, and Z. Derriche, "Sorption study of an acid dye from an aqueous solutions using modified clays," *Journal of Hazardous Materials*, vol. 119, no. 1–3, pp. 117–124, 2005.

[63] N. Gherbi, "Etude expérimentale et identification du processus de rétention des cations métalliques par des matériaux naturels," Thèse de Doctorat, Faculté des Sciences de l'Ingénieur, Université Constantine, Algérie, Africa, 2008.

[64] A. Talidi, "Etude de l'élimination du chrome et du bleu de méthylène en milieux aqueux par adsorption sur la pyrophyllite traitée et non traitée," Thèse de Doctorat, Université Mohammed V- Agdal, Rabat, Marocco, 2006.